Silicon (2019) 11:1817–1827
https://doi.org/10.1007/s12633-018-9997-7

ORIGINAL PAPER

Sulfonic Acid Functionalized SBA-3 Silica Mesoporous Magnetite Nanocomposite for Safranin O Dye Removal

Seyedeh Mahsa Seyed Danesh[1] · **Hossein Faghihian**[1] · **Shahab Shariati**[2]

Received: 19 August 2018 / Accepted: 9 October 2018 / Published online: 1 November 2018

Abstract

At the present study, sulfonic acid functionalized SBA-3 silica mesoporous magnetite nanocomposite (Fe_3O_4@SiO_2@SBA-3- SO_3H) was synthesized and its adsorption ability for removing Safranin O dye from aqueous samples was investigated. X-ray diffraction analysis (XRD), vibrating sample magnetometer (VSM), energy dispersive X-ray spectroscopy analysis (EDX), field emission scanning electron microscopy (FESEM) and Fourier transform infrared spectroscopy (FT-IR) were used to characterize the adsorbent. The FESEM images confirmed the synthesis of nanocomposites with good morphology and size below 30 nm. The experimental variables affecting the removal efficiency were optimized by Taguchi orthogonal array experimental design method (L_{16} array). At the optimal conditions (pH = 6, ionic strength = 0.005 mol L^{-1}, sample volume = 25 mL, adsorbent weight = 0.12 g and contact time = 15 min) the efficiency for Safranin O removal was obtained as higher than 91%. The pseudo-first-order, pseudo-second-order, intra particle and Elovich kinetic models were investigated, and the kinetic data followed the pseudo-second-order kinetic model (R^2 = 0.9999). Also, the study of three isotherm models (Langmuir, Freundlich and Temkin) showed that Freundlich isotherm was suitable for describing Safranin O adsorption (R^2 = 0.9941, n = 1.428). The reusability experiments showed high removal efficiency of Safranin O after 9 cycles of usage. Finally, the results of Safranin O removal from the aqueous real samples showed the applicability of this nanocomposite for Safranin O removal applications.

Keywords Nanocomposite · Taguchi · Removal · Safranin O · Magnetite · Mesopore · SBA

1 Introduction

Contamination of water by dyes that are consumed in many industries is an important environmental problem because it threatens health of humans and aquatic organisms [1, 2]. It has been reported that 10,000 different dyes are produced annually for different industrial activities [3]. Many of these dyes are toxic and dangerous for aquatic life organisms. Also, release of dye compounds into the water system is hazardous for human and can cause mutagenic effects, allergic dermatitis, skin irritation, cancer, and mutation [4, 5]. For removing dyes from aqueous solutions, physical and chemical methods such as flocculation, electro-flotation, precipitation, electro-kinetic coagulation, ion exchange, membrane filtration, electrodialysis, photocatalytic degradation, oxidation, irradiation, and ozonation have been used [6–8]. Safranin O (3,7-dimethyl-10-phenylphenazin-10-ium-2,8-diamine chloride) as an oldest synthetic dye is reddish brown powder and water-soluble [9]. It is widely used in flavoring and coloring candies and cookies as food dye as well as for dyeing tannin, cotton, bast fibers, wool, silk, leather and paper [10, 11]. Safranin O has a lot of harm for human health such as irritation to mouth, throat, tongue, lips and pain in stomach even causes diarrhea, vomiting and nausea [12, 13]. Moreover, it leads to eye irritation that even cause damage the cornea and conjunctiva [14, 15]. The various methods

✉ Shahab Shariati
shariaty@iaurasht.ac.ir

[1] Department of Chemistry, Shahreza Branch, Islamic Azad University, Shahreza, Iran

[2] Department of Chemistry, Rasht Branch, Islamic Azad University, Rasht, Iran

were used for removing this dye from wastewater like coagulation, flocculation, reverse osmosis, and adsorption onto several adsorbent materials [16, 17]. Up to now, different types of adsorbent materials have been successfully investigated for the removal of various dyes [18–28]. In this study, Fe_3O_4@SiO_2@SBA-3-SO_3H nanocomposite was synthesized and used as an adsorbent to remove Safranin O from aqueous samples. After characterization of the synthesized nanocomposite, kinetic and isotherm models were studied to clarify the adsorption process. Also, Taguchi experimental design was examined to determine the optimum conditions of the experiment.

2 Experimental

2.1 Materials and Instruments

All of chemicals used including ferric chloride hexahydrate ($FeCl_3.6H_2O$), ferrous chloride tetrahydrate ($FeCl_2.4H_2O$), ammonia solution (28%, w/w), hydrochloric acid (37%, w/w), cetyl trimethyl ammonium bromide (CTAB), ethanol, sodium chloride, tetraethyl orthosilicate (TEOS), mercaptopropyl trimethoxysilane (MPTS) and Safranin O were purchased with high purity from Merck (Darmstadt, Germany) and Sigma-Aldrich (ST. Louise, Missori, USA). FT-IR spectra of samples were determined using Shimadzu FT-IR spectrophotometer (model 470, Japan) by using KBr pellets. An Agilent UV-Vis spectrophotometer (Carry 60, USA) was used for spectrophotometric measurements. The XRD analysis of the synthesized nanocomposite was studied by Phillips X-ray diffractometer (pw-1840) with Cu-Kα radiation source ($\lambda = 1.54056°$). The morphologies of the as-synthesized particles were analyzed by FESEM (MIRA3, TE-SCAN Co., Czechoslovakia). VSM instrument (LBKFB model- Meghnatis Daghigh, Kavir Co.,) was used to investigate the magnetic property of the synthesized nanocomposite. Energy dispersive X-ray spectroscopy analysis (EDX) was carried out using a FESEM (Sigma VP, ZEISS company, Germany) equipped to EDS detector and was used to confirm the elemental composition of the synthesized nanocomposites. A digital Bante pH meter (model 930, China) was used to adjust the pH values of the solutions. Digital ultrasound (DSA100-SK2 code, DIY brand, China) and oven (Memert, Germany) were utilized. For magnetic separations, a strong super magnet ($1 \times 3 \times 5$ cm) with 1.4 Tesla magnetic field was applied.

2.2 Synthesis of Magnetite Nanoparticles (Fe_3O_4)

The co-precipitation method was applied for the synthesis of magnetite nanoparticles (MNPs). Briefly, 10.4 g of $FeCl_3.6H_2O$, 4.0 g of $FeCl_2.4H_2O$ and 1.7 mL of HCl 37% (w/w) were dissolved in distilled water and the solution was adjusted to the mark of a 50 mL volumetric flask. Afterward, the solution was transfered into a separatory funnel and degassed for 20 min using nitrogen gas.

Then, 250 mL of 1.5 mol L^{-1} ammonia solution was transferred into a three necked flask containing a magnet. This solution was heated to 80 °C in the oil bath. Thereafter, the mixture of iron chlorides was added dropwise to a solution of ammonia in a degassed environment during 60 min. When the first drop entered, the nucleation process was started and black nanoparticles of Fe_3O_4 sediment was formed. After the reaction was completed, the MNPs were washed with double distilled water four times and were separated from the reaction environment with a strong super magnet (1.4 T). The synthesized MNPs were located in 0.1 mol L^{-1} NaOH solution during 24 hours due to prevent the accumulation of MNPs. Eventually, MNPs washed with distilled water and were dried at 120 °C for 120 min in the oven [29].

2.3 Surface Modification of the MNPs with Silica Coating (Fe_3O_4@SiO_2)

The surface of produced MNPs was modified with silica coating for increasing their stability against oxidation and other side reactions. For silica coating the following steps were applied:

200 mL of the suspension of MNPs (2.4 g of MNPs in 600 mL ethanol 96%) was added to a 1 L volumetric flask and was put in an ultrasonic bath for 10 min at 80 °C. Afterwards, 25 mL of ammonia solution (28% w/w) was added to the suspension (solution A).

On the other hands, 100 mL of pure ethanol and 10.8 mL of TEOS were mixed (solution B). The solution B was added to a solution A during 2 h using a separatory funnel. After that, the mixture was stirred strongly for 7 h under the same conditions. Then, the mixture was separated by magnet and washed three times with 1:1 mixture of distilled water/ethanol. The produced brown sediment was dried at 100 °C for 5 h [30, 31].

2.4 Synthesis of Santa Barbara Amorphous Mesoporous Magnetite Nanoparticles (Fe_3O_4@SiO_2@SBA-3)

Synthesis of Santa Barbara Amorphous (SBA-3) mesoporous structure on the surface of Fe_3O_4@SiO_2 nanoparticles was carried out according to our previous study [29]. First, 4.1 g of CTAB surfactant was dissolved into distilled water (35 mL) in a beaker and was stirred for 10 min at 35 °C. Then, 2.5 mL of concentrated HCl was added to the

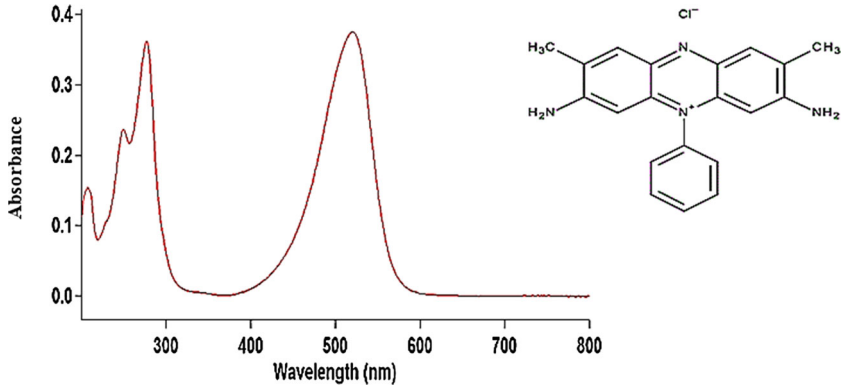

Fig. 1 Absorption spectra of Safranin O dye

mixture and was stirred for 1 h. Afterward, 1.5 g of prepared magnetite nanoparticles with silica coating (Fe_3O_4@SiO_2) was added to the mixture and stirred for 20 min. In the next step, 4 mL of TEOS was added to the mixture and stirred for 0.5 h in the same conditions. The mixture was washed several times with distilled water to remove HCl from the environment. In the end, the obtained precipitate was washed with distilled water and was separated by the magnet. This product dried in an oven at 100 °C for 12 h. The dried precipitate was transferred into a jelly balloon and added to 100 mL of ethanol. The dried precipitate was poured into a volumetric flask and 100 mL of ethanol was added to it and refluxed for 6 h. After time period of reflux, the content of the container was washed with double distilled water (5 times), separated with the magnet and dried in an oven at 90 °C. Then, the nanoparticles were placed in the furnace for 5 h to calcify at 550 °C. The color of the final product was orange [32].

2.5 Synthesis of Fe_3O_4@SiO_2@SBA-3 Functionalized with Sulfonic Acid Group (Fe_3O_4@SiO_2@SBA-3-SO_3H)

For this purpose, 1 g of synthesized Fe_3O_4@SiO_2@SBA-3 nanoparticles and 1.25 mL of MPTS were added to 30 mL of toluene and the mixture was stirred. Then, the mixture was refluxed for 24 h at 130 °C. The mixture was washed with distilled water and separated by a magnet. Eventually, it dried in the oven at 90 °C. 2 mL of hydrogen peroxide and 20 mL of methanol were added to nanoparticles and the mixture was stirred at 25 °C for 24 h. Finally, the nanoparticles were washed with double distilled water, separated by a magnet and dried in an oven at 90 °C for 2 h [31].

Table 1 Factors and levels of Taguchi experimental design

Parameter	Level 1	Level 2	Level 3	Level 4
pH	3	4	5	6
Ionic strength (mol L^{-1})	0	0.005	0.01	0.05
Contact time (min)	5	10	15	30
Volume of solution (mL)	25	50	75	100
Weight of adsorbent (g)	0.01	0.05	0.08	0.12

2.6 Preparation of Safranin O Solutions

In this study, magnetic nanoparticles (Fe_3O_4@SiO_2@SBA-3-SO_3H) were used to remove Safranin O dye from aqueous samples. For this purpose, 1000 mg L^{-1} of Safranin O was prepared in distilled water and by diluting it, the desired concentrations were prepared. Initially, to determine the dependence of UV-Vis absorption behavior of Safranin O on the pH of the solution, solutions containing 10 mg L^{-1} of Safranin O were prepared in the pH range of 2 to 10. As shown in Fig. 1, maximum absorption wavelength of the Safranin O was obtained as 517 nm.

2.7 Experimental Design Method to Remove Safranin O

In this study, five experimental variables affecting the extraction efficiency including adsorbent weight, adsorbent contact time with solution (stirring time), ionic strength, pH, and volume of dye solution were investigated in four levels using Taguchi experimental design (Table 1). 16 experiments were carried out to determine the optimum conditions for the test. Briefly, for each removal experiment, the certain amount of dye solution was poured into the beaker and after pH adjustment, its initial UV-Vis absorption was measured using the spectrophotometer. Then, adsorbent was added to the beaker and the mixture was stirred for a specific time. After completion of removal period, the beaker was placed on a magnetic stirrer, the MNPs were separated and the absorption of residual solution was

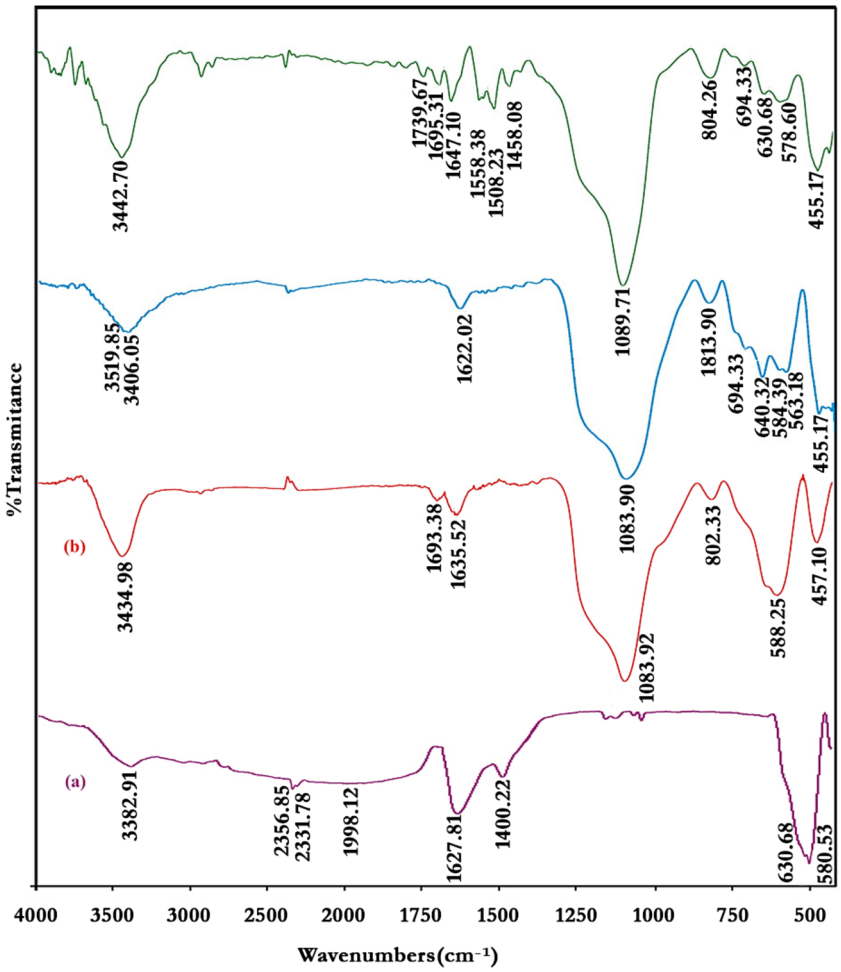

Fig. 2 FT-IR spectra of **a** Fe_3O_4, **b** Fe_3O_4@SiO_2, **c** Fe_3O_4@SiO_2@SBA-3 **d** Fe_3O_4@SiO_2@SBA-3/SO_3H

measured spectrophotometry. The dye removal efficiency was calculated according to Eq. 1.

$$\%\ \text{Removal} = \frac{C_0 - C_t}{C_0} \times 100 \quad (1)$$

Where, C_o and C_t are the initial and equilibrium concentrations of Safranin O dye after adsorption process, respectively.

3 Results and Discussion

3.1 Characterization of the Synthesized Nanocomposites

Figure 2 shows the FT-IR spectrum of Fe_3O_4, Fe_3O_4@SiO_2, Fe_3O_4@SiO_2@SBA-3 and Fe_3O_4@SiO_2@SBA-3/SO_3H. Fig. 2a displays FT-IR spectra of Fe_3O_4 MNPs. The absorption band in the region of 500–600 cm^{-1} is related to the Fe-O vibrating bands. This absorption band is observed in all spectra and because of its coating with the silica layer, its intensity is reduced in the spectra of (b) to (d). Part (b) shows the FT-IR spectrum of Fe_3O_4@SiO_2 MNPs. The observed peaks in 1083 and 699 cm^{-1} are related to asymmetric and symmetric vibrations of Si-O-Si which is shown in (b) to (d). The absorption band at 1820 cm^{-1} is related to the stretching vibrations of S-OH. Width peak at 3000 to 3500 cm^{-1} is related to adsorbed water molecules. Part (c) represents the spectrum of Fe_3O_4@SiO_2@SBA-3 and it shows that the intensity of the peaks in this spectrum is reduced. Also, the spectrum of Fe_3O_4@SiO_2@SBA-3/SO_3H is shown in part (d). The peaks of symmetric and asymmetric stretching vibrations of O=S=O and the S-O from the SO_3H group are observed in 1200-1250, 980-1100 and 628 cm^{-1}, respectively. O=S=O peaks indicate overlap with the Si-O-Si peak.

Figure 3a shows the XRD spectrum of Fe_3O_4@SiO_2@SBA-3. In (a), the two peaks are in 2θ equal to 1° and 0.84° in the range of 0–2. This represents the hexagonal structure of the cavities for the magnetic combination of the SBA-3. In (b), appeared peaks in 2θ are equal to 35.66°, 43.35°, 57.3° and 62.96° related to Fe_3O_4 nanoparticles that displays the XRD pattern of the reference for the Fe_3O_4 standards (19-629 JCPDS).

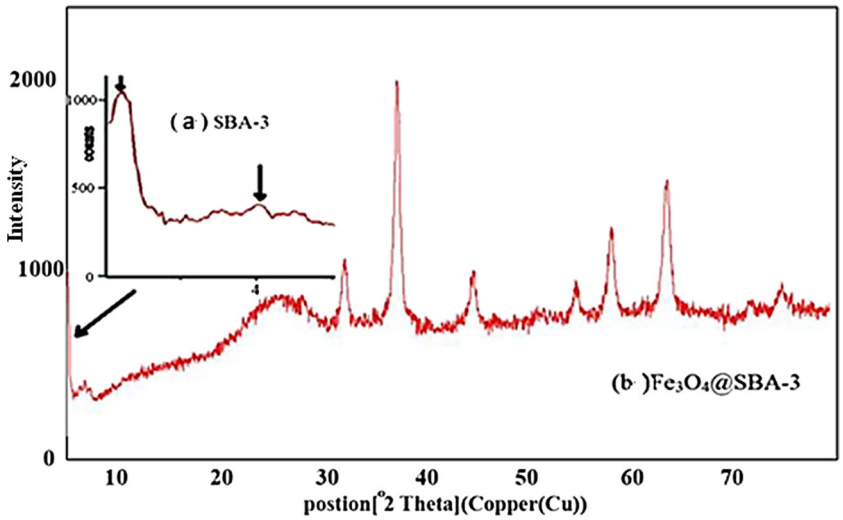

Fig. 3 The XRD spectra of Fe_3O_4@SiO_2@SBA-3 **a** Low angles **b** High angles

Figure 4 shows the EDX image for the identification of Fe_3O_4@SiO_2@SBA-3 nanocomposite. The spectrum confirms the presence of Fe (32.50%), O (38.13%) and Si (29.37%) elements in the nanocomposite structure that shows the presence of 44.8% wt of Fe_3O_4 in the structure of synthesized nanocomposite.

Figure 5 indicates the FESEM image of the synthesized Fe_3O_4@SiO_2@SBA-3 nanocomposite. This figure shows that the particle size is less than 30 nm.

The vibrating scanning magnetometry intensity (VSM) of Fe_3O_4, Fe_3O_4@SiO_2 and Fe_3O_4@SiO_2@SBA-3 magnetic nanoparticles are demonstrated in Fig. 6. The magnitude of their magnetic properties are obtained as 55, 40, and 30 emg /u, respectively. Reducing the magnetic properties of the mesoporous coated magnetite relative to bare magnetite nanoparticles are due to the coating of Fe_3O_4 magnetic particles with non-magnetic SBA-3 and SiO_2 shell. In addition, the magnetic property of Fe_3O_4@SiO_2@SBA-3 is lower than that of Fe_3O_4@SiO_2, because magnetic property gets less by adding the SBA-3 layer to Fe_3O_4@SiO_2. The experiments showed that the samples are easily separated from the water solution by the magnet within short time.

The surface area and pore size of the Fe_3O_4@SiO_2@SBA-3 nanoparticles were measured in our previus study by nitrogen adsorption–desorption isotherms (at 77 K) and BET method as 627.87 m^2g^{-1} and 2.44 nm, respectively [29].

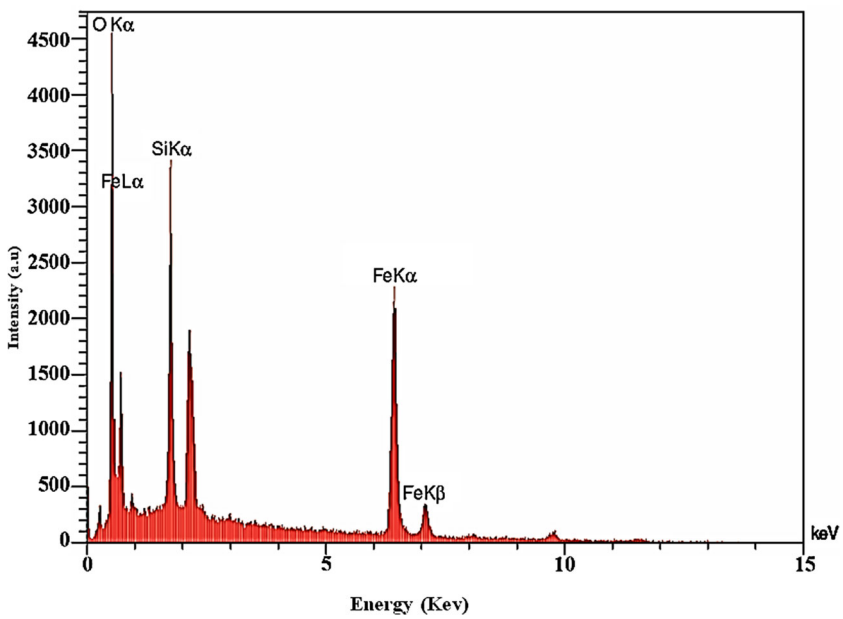

Fig. 4 The EDX spectrum of Fe_3O_4@SiO_2@SBA-3/SO_3H

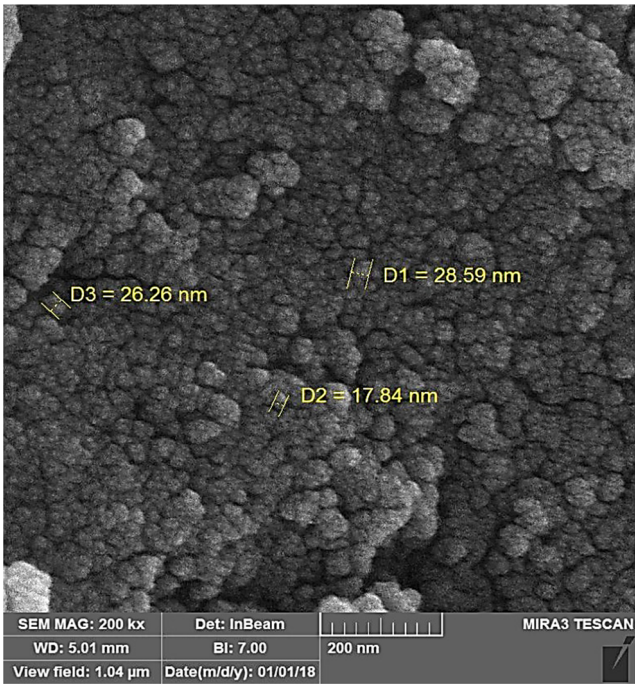

Fig. 5 FESEM image of Fe_3O_4@SiO_2@SBA-3 nanocomposite

3.2 Effect of Solution pH on the Efficiency of Safranin O Removal

In preliminary studies, alkaline and acidic pHs were investigated in the pH range of 3–10 using HCl (1 mol L^{-1}) and NaOH (1 mol L^{-1}) solutions. The preliminary experiments showed the better removal efficiency of Safranin O under pHs lower than 6. Therefore, pHs between 3 to 6 were investigated in optimization step. As shown in Fig. 7a, the highest dye adsorption was obtained at pH = 6. Therefore, this pH was chosen as the optimum value for other experiments.

3.3 Effect of Ionic Strength on the Efficiency of Safranin O Removal

The effect of ionic strength on the dye removal was investigated by adding different concentrations of NaCl to solution. Initially, with the increase of ionic strength, amount of dye removal increased due to the salting out effect. Furthermore, by more increasing in ionic strength, the amount of dye removal has gradually decreased due to the competition between Na^+ and Safranin O dye for adsorption sites. According to the results in Fig. 7b, the salt concentration of 0.005 mol L^{-1} was obtained as the optimum amount of salt for ion strength adjustment.

3.4 The Effect of Contact Time on the Efficiency of Safranin O Removal

To investigate the effect of contact time between the adsorbent and solution, contact times of 5, 10, 15 and 30 min were studied. As shown in Fig. 7c, the adsorption process was rapid and finally, the system reached to equilibrium

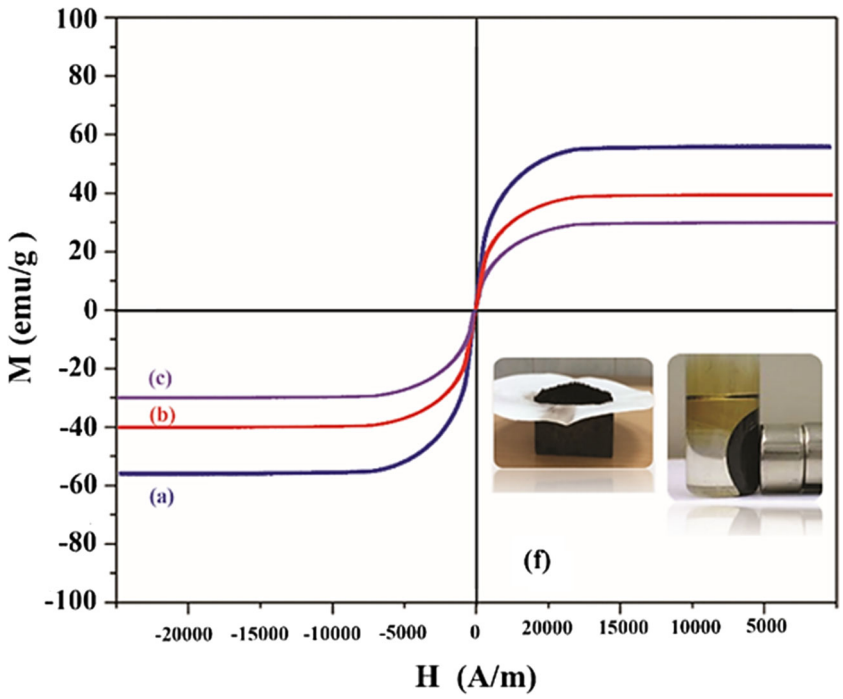

Fig. 6 Results of the VSM curve for identification of **a** Fe_3O_4, **b** Fe_3O_4@SiO_2, **c** Fe_3O_4@SiO_2@SBA-3

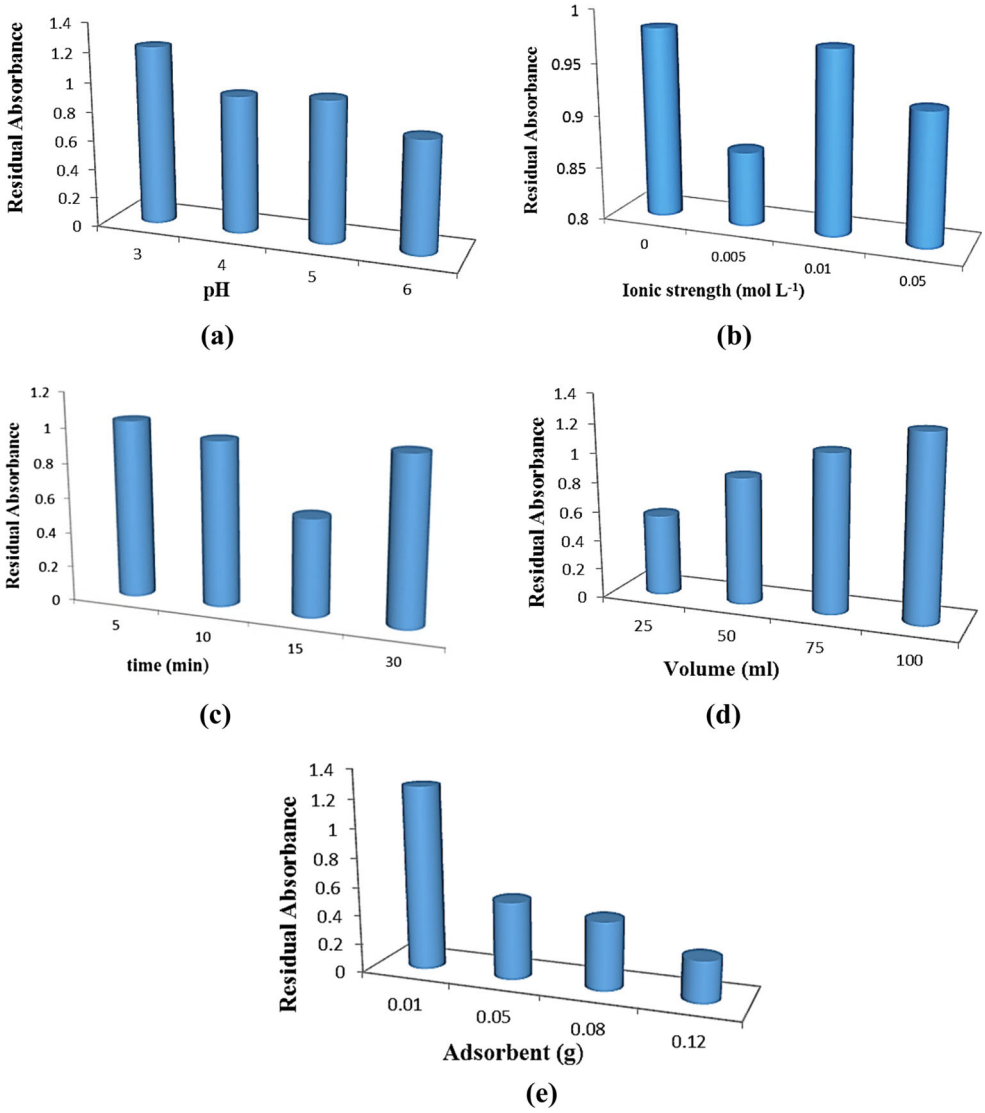

Fig. 7 **a** Effect of pH, **b** effect of ionic strength, **c** effect of contact time, **d** effect of volume of sample and **e** effect of weight of adsorbent on the efficiency of removal Safranin O

after 15 min. This time is less than similar investigations on Safranin O dye adsorption [33].

3.5 The Effect of Volume of Sample on the Efficiency of Safranin O Removal

Figure 7d displays that with increasing of sample volume from 25 to 100 mL, the percentage of dye removal decreased. Therefore, the volume of 25 mL was selected as optimal volume. Afterwards, the amount of dye removal was reduced by increasing the volume of the solution. With increasing volume at constant concentration, the amount of dye increases. At higher volumes of sample, more mass of Safranin O is present in the sample and at a constant weight of adsorbent, the adsorption sites of adsorbent is not enough for complete removal.

3.6 The Effect of Adsorbent Weight on the Efficiency of Dye Removal

According to the results of the experiments in Fig. 7e, the dye removal is increased by increasing the amount of adsorbent. Hence, 0.12 g of adsorbent (4.8 g L^{-1}) was considered as the optimum adsorbent weight for dye removal.

3.7 Approval Test in Optimal Conditions for Removing Safranin O

To investigate the accuracy of the optimum values obtained by Taguchi orthogonal array for removing Safranin O dye, five experiments were carried out under the optimum conditions (initial Safranin O concentration= 25 mg L^{-1}, ionic strength = 0.005 mol L^{-1}, pH 6, adsorbent weight

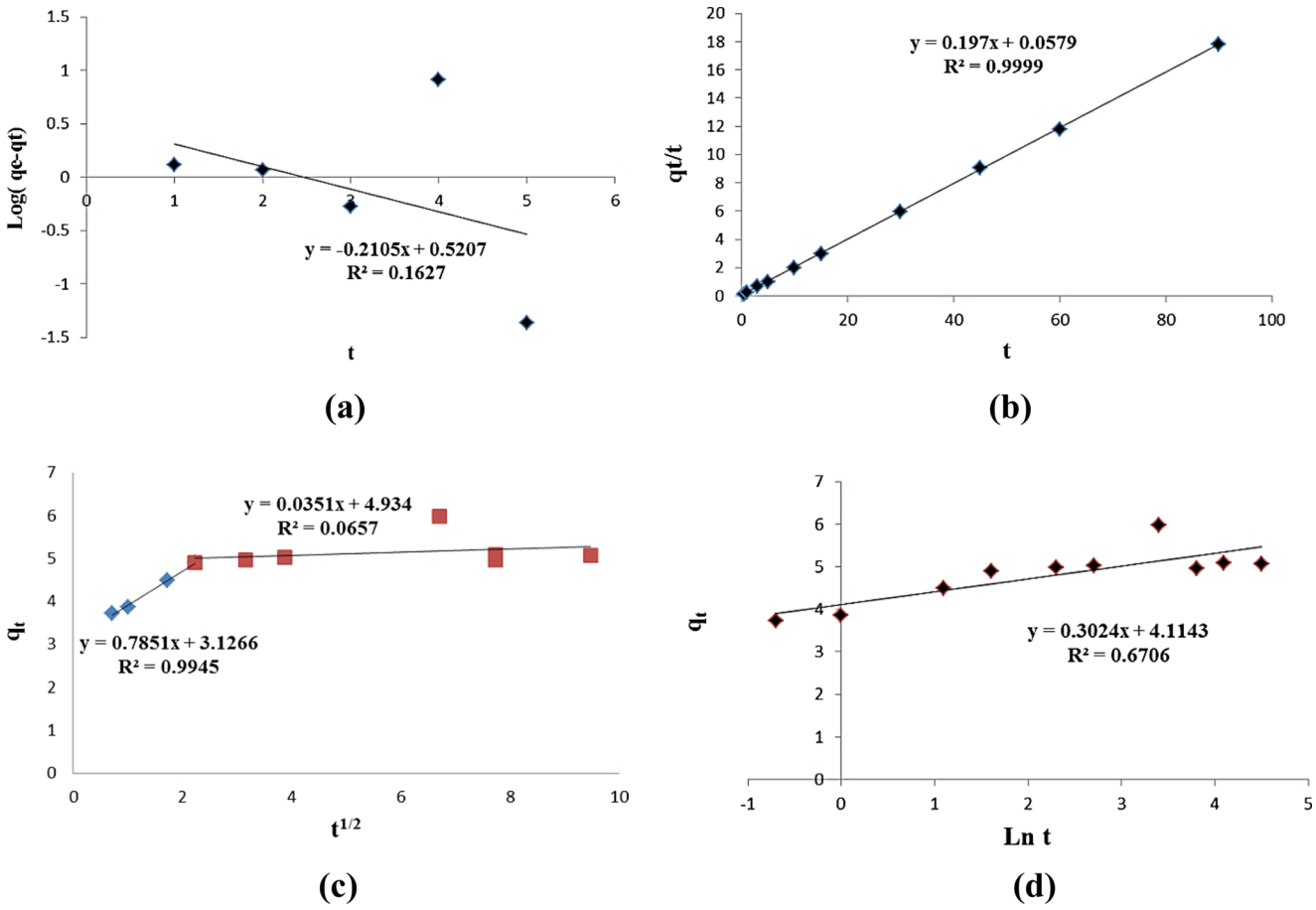

Fig. 8 **a** pseudo-first-order kinetic, **b** pseudo-second-order kinetic, **c** Intra-particle diffusion and **d** Elovich models for removal Safranin O

=0.12 g, contact time = 15 min and sample volume = 25 mL). The results showed that under optimum conditions, the removal efficiency is higher than 94.5% (S_D = 0.436 for five removal replicates in optimum conditions) with relative standard deviation percent (RSD %) of 0.462 that indicates the process of Safranin O removal by the proposed adsorbent is repeatable.

3.8 Investigating of Kinetic Models

To examine the rate of the adsorption process and rate controlling step, kinetic models are used. Pseudo first order, pseudo second order, Elovich and intra-particle diffusion are the most kinetic models [34]. In the present study, these kinetic models were used for studying adsorption kinetic behavior of Safranin O on Fe_3O_4@SiO_2@SBA-3/SO_3H adsorbent. Using Eq. 2 related to the pseudo- first -order, the values of q_e, q_t, and K_1 were calculated, which q_e and q_t are the amount of dye adsorbed (mg g^{-1}) at equilibrium time and at the time t, respectively. The curve corresponding to first order kinetic model is shown in Fig. 8a. The correlation coefficient of this model is undesirable (R^2 = 0.1627). So, the empirical data does not follow the pseudo first order kinetic model.

$$\log (q_e - q_t) = \log q_e - \frac{k_1.t}{2.303} \quad (2)$$

Table 2 The obtained parameters of kinetic models for removal of 25 mg L^{-1} of Safranin O

Kinetic model	Pseudo first order			Pseudo second order			Intraparticle diffusion			Elovich		
Parameter	q_e	K_1	R^2	q_e	K_2	R^2	K	C	R^2	α	β	R^2
Concentration (25 mgL^{-1})	5.980	−0.210	0.1627	5.076	0.670	0.9999	0.143	4.177	0.485	156227.660	3.309	0.6702

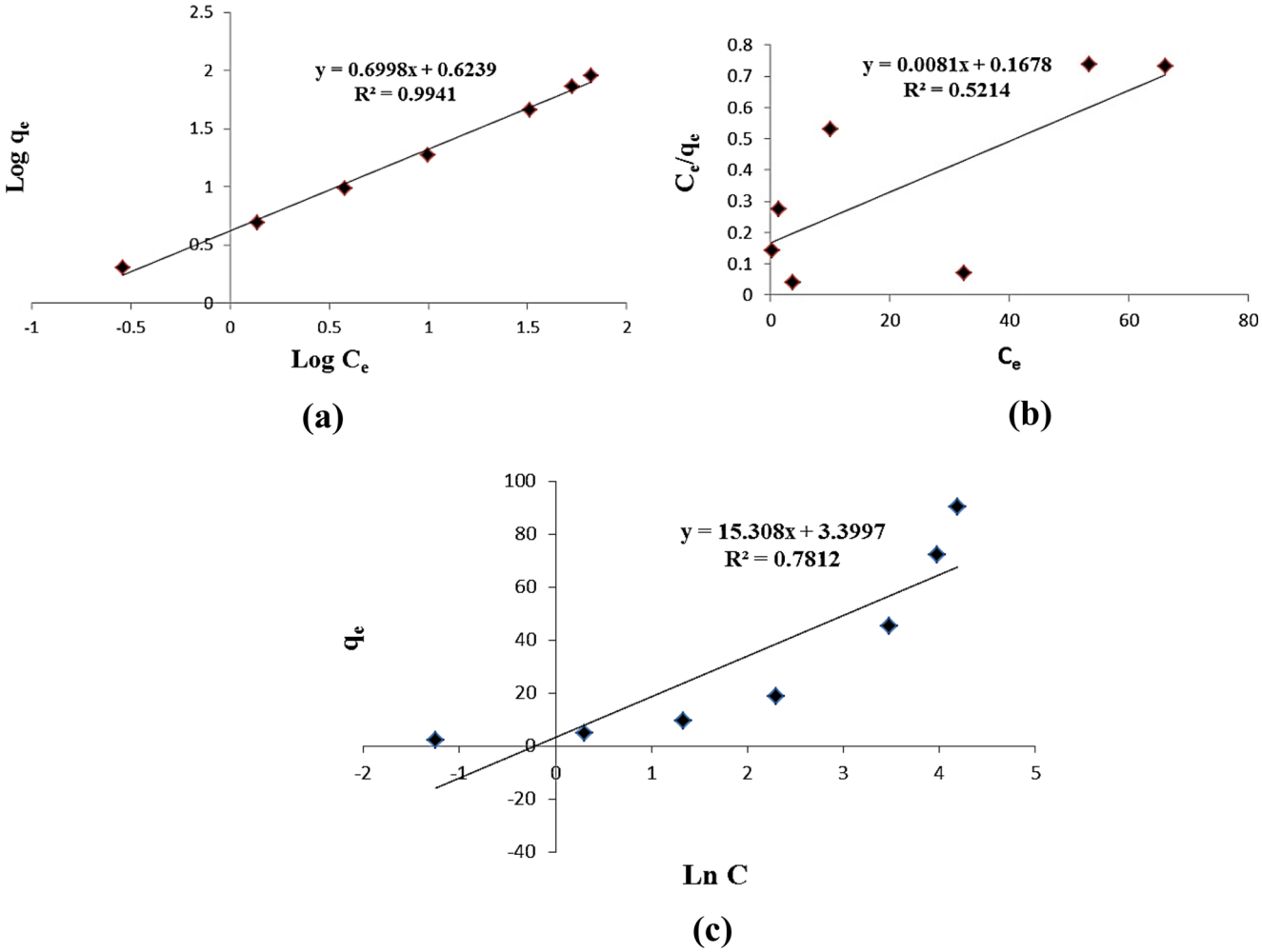

Fig. 9 **a** Freundlich, **b** Langmuir and **c** Temkin isotherms to remove Safranin O

On the other hand, the pseudo second order kinetic equation is shown as follows (3):

$$\frac{t}{q_t} = \frac{1}{k_2 q_e^2} + \left(\frac{1}{q_e}\right).t \tag{3}$$

Where k_2 is the equilibrium rate constant (g mg^{-1} min^{-1}). As shown in Fig. 8b, the correlation coefficient of this model was obtained as $R^2 = 0.9999$. Therefore, this model is suitable for the interpretation of empirical data. It shows that adsorption of dye on the synthesized adsorbent is chemical. Also, intra-particle diffusion model was investigated, which equation related to it is given as:

$$q_t = k_{diff} t^{1/2} + C \tag{4}$$

Where K_{diff} is the intra-particle diffusion rate constant (mg g^{-1} $h^{1/2}$) and C (mg g^{-1}) is the thickness of the boundary layer. The obtained result of this model is shown in Fig. 8c. The model shows that intra-particle diffusion is not the only stage for determining speed [35].

The other studied kinetic model is Elovich that its equation is shown in Eq. 5.

$$q_t = 1/\beta.\ln(\alpha.\beta) + 1/\beta.\ln(t) \tag{5}$$

Table 3 The obtained parameters of isotherm models for removal of Safranin O

Langmuir			Freundlich			Temkin		
q_m	K_l	R^2	K_f	n	R^2	K_t	K_l	R^2
123.45	0.048	0.5214	4.206	1.428	0.9941	1.248	15.308	0.7812

Table 4 Results of adsorbent efficacy on the removal of Safranin O in real samples

Sample[a]	Sample absorption before adding dye	Absorption of dye solution	Sample absorption after dye removal	Recovery (%)
Water of dye industry	0.004	1.482	0.194	91.653
Water of Pasikhan river	0.007	1.393	0.153	93.262
Tap water	0.001	1.427	0.091	98.211

[a]Samples were collected from Rasht city, Guilan Province, Iran

Where α is the initial sorption rate (mg g^{-1} min^{-1}) and β is the extent of surface coverage and activation energy of chemical adsorption (g mg^{-1}). According to Fig. 8d and its correlation coefficient, it can be concluded that its sorption data does not follow the Elovich kinetic model (Table 2).

3.9 Study of the Adsorption of Safranin O Isotherms

The obtained results in adsorption of Safranin O using Langmuir, Freundlich and Tamkin isotherms were studied in concentration range of 10–500 mg L^{-1} of Safranin O dye. Langmuir equation is shown in Eq. 6.

$$\frac{c_e}{q_e} = \frac{1}{k_l q_m} + \frac{c_e}{q_m} \tag{6}$$

Where c_e and q_e are the equilibrium concentration of the Safranin O solution (mg L^{-1}) and the amount of adsorbed dye per gram of adsorbent (mg g^{-1}), respectively. K_l displays the energy of correlation (L mg^{-1}) and q_m is the maximum adsorption capacity (mg g^{-1}).

The Freundlich isotherm is obtained from the following equation:

$$\text{Log } q_e = \log\ (k_f) + \frac{1}{n}\log(C_e) \tag{7}$$

Where q_e is the amount of adsorbed Safranin O in equilibrium condition (mg g^{-1}), k_f, n and C_e are capacity of adsorption, intensity of adsorption and equilibrium concentration, respectively.

Temkin isotherm can be presented by the Eq. 8:

$$q_e = k_1 \text{Ln}(k_2) + k_1 \text{Ln}(C_e) \tag{8}$$

Where k_1 (L g^{-1}) and k_2 (Kj mol^{-1}) are constants of the isotherm, respectively.

The Freundlich isotherm with $R^2 = 0.9941$ shows the best interpretation of the results. It can be concluded that the adsorption process is multi-layered. The results are presented in Fig. 9 and Table 3.

3.10 Investigating the Reusability of Adsorbent for Safranin O Removal

The adsorbent recycling is an important case that reduces the removal cost and waste production. For recycling the Fe_3O_4@SiO_2@SBA-3/SO_3H adsorbent, 0.1 M HCl solution was used to desorb Safranin O dye from the surface of nanocomposite. After washing the synthesized adsorbents, the adsorbent was used for 10 repetitious adsorption process at optimum conditions. The results show that adsorbent keep its ability after nine removal process with removal efficiency higher than 90%.

3.11 Safranin O Adsorption from Real Samples

To investigate the ability of synthesized nanoparticles to remove Safranin O, water samples from a dye industry, Pasikhan river and tap water were collected from Rasht city (Guilan Province, Iran) and used for investigating the dye removal efficiency via spiking Safranin O to their matrix. The results of Safranin O removal from each spiked sample are summarized in Table 4.

4 Conclusion

In this study, Fe_3O_4@SiO_2@SBA-3/SO_3H MNCs were synthesized and their ability for removal of Safranin O cationic dye was investigated. The results showed the proposed adsorbent is an efficient adsorbent for removing this dye. The kinetic results suggested that the pseudo-second-order kinetic model is the best kinetic model for interpretation of results respect to three others. Also, the results showed that Langmuir isotherm is a suitable model for experimental data. Based on the results of this study, it can be concluded that the Fe_3O_4@SiO_2@SBA-3/SO_3H is a potential adsorbent for removal of Safranin O dye from the aqueous solutions.

Acknowledgements The authors are grateful to Rasht Branch, Islamic Azad University and International Association of Science Parks (IASP) of Guilan Province for their support.

References

1. Ghaedi M, Pakniat M, Mahmoudi Z, Hajati S, Sahraei R, Daneshfar A (2014) Synthesis of nickel sulfide nanoparticles loaded on activated carbon as a novel adsorbent for the competitive

removal of Methylene blue and Safranin-O. Spectrochim Acta Part A 123:402–409
2. Baskaralingam P, Pulikesi M, Elango D, Ramamurthi V, Sivanesan S (2006) Adsorption of acid dye onto organobentonite. J Hazard Mater B 128:138–144
3. Chowdhury Sh, Mishra R, Kushwaha P, Saha P (2012) Removal of safranin from aqueous solutions by NaOH-treated rice husk: thermodynamics, kinetics and isosteric heat of adsorption. Asia-Pac J Chem Eng 7:236–249
4. Kumar Sahu M, Kishore Patel R (2015) Removal of safranin-O dye from aqueous solution using modified red mud: kinetic and equilibrium studies. RSC Adv 5:78491–78501
5. Gupta VK, Mittal A, Jain R, Mathur M, Sikarwar Sh (2006) Adsorption of Safranin-T from wastewater using waste materials activated carbon and activated rice husks. J Colloid Interface Sci 303:80–86
6. Mohagheghian A, Karimi S-A, Yang J-K, Shirzad-Siboni M (2015) Photocatalytic degradation of a textile dye by illuminated tungsten oxide nanopowder. J Adv Oxid Technol 18(1):61–68
7. Shirzad-Siboni M, Khataee A, Vahid B, Joo SW, Fallah S (2014) Preparation of a Green photocatalyst by immobilization of synthesized ZnO nanosheets on scallop shell for degradation of an azo dye. Curr Nanosci 10(10):684–694
8. Shirzad-Siboni M, Samarghandi M, Yang J-K, Lee S-M (2011) Photocatalytic removal of Reactive Black-5 dye from aqueous solution by UV irradiation in aqueous TiO_2: equilibrium and kinetics study. J Adv Oxid Technol 14:302–307
9. Kaur S, Rani S, Mahajan RK, Asif M, Kumar Gupta V (2015) Synthesis and adsorption properties of mesoporous material for the removal of dye safranin: kinetics, equilibrium, and thermodynamics. J Ind Eng Chem 22:19–27
10. Zaghbani N, Hafiane A, Dhahbi M (2008) Removal of Safranin T from wastewater using micellar enhanced ultrafiltration. Desalination 222:348–356
11. Chandane V, Singh VK (2014) Adsorption of safranin dye from aqueous solutions using a low-cost agro-waste material soybean hull. Desalin Water Treat 57:1–13
12. Khan TA, Khan EA (2015) Shahjahan, Removal of basic dyes from aqueous solution by adsorption onto binary iron-manganese oxide coated kaolinite: non-linear isotherm and kinetics modeling. Appl Clay Sci 107:70–77
13. Chowdhury Sh (2011) Adsorption kinetic modeling of safranin onto rice husk biomatrix using pseudo-first- and pseudosecond-order kinetic models: comparison of linear and non-linear methods. Clean: Soil, Air, Water 39:274–282
14. Alipanahpour Dil E, Ghaedi M, Asfaram A, Mehrabi F, Bazrafshan AA, Ghaedi AM (2016) Trace determination of safranin O dye using ultrasound assisted dispersive solid phase micro extraction: artificial neural network-genetic algorithm and response surface methodology. Ultrason Sonochem 33:129–140
15. Fayazi M, Afzali D, Taher MA, Mostafavi A, Gupta VK (2015) Removal of Safranin dye from aqueous solution using magnetic mesoporous clay: optimization study. J Mol Liq 212:675–685
16. El Haddad M, Regti A, Slimani R, Lazar S (2014) Assessment of the biosorption kinetic and thermodynamic for the removal of safranin dye from aqueous solutions using calcined mussel shells. J Ind Eng Chem 20:717–724
17. El Haddad M, Slimani R, Mamouni R, Laamari MR, Rafqah S, Lazar S (2013) Evaluation of potential capability of calcined bones on the biosorption removal efficiency of safranin as cationic dye from aqueous solutions. J Taiwan Inst Chem Eng 44:13–18
18. Keyhanian F, Shariati Sh, Faraji M, Hesabi M (2016) Magnetite nanoparticles with surface modification for removal of methyl violet from aqueous solutions. Arab J Chem 9:S348–S354
19. Mahmoodi NM, Najafi F (2012) Synthesis, amine functionalization and dye removal ability of titania/silica nano-hybrid. Micropor Mesopor Mat 156:153–160
20. Shariati Sh, Faraji M, Yamini Y, Rajabi AA (2011) Fe_3O_4 magnetic nanoparticles modified with sodium dodecyl sulfate for removal of safranin O dye from aqueous solutions. Desalination 270:160–165
21. Ghaedi M, Hassanzadeh A, Nasiri Kokhdan S (2011) Multiwalled carbon nanotubes as adsorbents for the kinetic and equilibrium study of the removal of alizarin Red S and Morin. J Chem Eng Data 56:2511–2520
22. Alizadeh N, Shariati Sh, Besharati N (2017) Adsorption of crystal violet and methylene blue on azolla and fig leaves modified with magnetite iron oxide nanoparticles. Int J Environ Res 11(1):197–206
23. Gutierrez-Segura E, Solache-Rios M, Colin-Cruz A (2009) Sorption of indigo carmine by a Fe-zeolitic tuff and carbonaceous material from pyrolyzed sewage sludge. J Hazard Mater 170:1227–1235
24. Shirzad-Siboni M, Khataee A, Vafaei F, Joo SW (2014) Comparative removal of two textile dyes from aqueous solution by adsorption onto marine-source waste shell: kinetic and isotherm studies, Korean. J Chem Eng 31(8):1451–1459
25. Farrokhi M, Hosseini S-C, Yang J-K, Shirzad-Siboni M (2014) Application of ZnO-Fe3O4 nanocomposite on the removal of Azo dye from aqueous solutions: kinetics and equilibrium studies. Water Air Soil Pollut 225:1–12
26. Ehyaee M, Safa F, Shariati Sh (2017) Magnetic nanocomposite of multi-walled carbon nanotube as effective adsorbent for methyl violet removal from aqueous solutions: response surface modeling and kinetic study. Kor J Chem Eng 34(4):1051–1061
27. Bandari F, Safa F, Shariati S (2015) Application of response surface method for optimization of adsorptive removal of eriochrome black T using magnetic multi-wall carbon nanotube nanocomposite. Arab J Sci Eng 40:3363–3372
28. Sojoudi M, Shariati Sh, Khabazipour M (2016) Amine functionalized kit-6 mesoporous magnetite nanocomposite as an efficient adsorbent for removal of Ponceau 4R dye from aqueous solutions. Anal Bioanal Chem 3(1):287–298
29. Khabazipour M, Shariati Sh, Safa F (2016) SBA and KIT-6 mesoporous silica magnetite nanoparticles: synthesis and characterization. Synth React Inorg Met Org Chem 46:759–765
30. Khabazipour M, Shariati Sh (2014) Synthesis and characterization of amine functionalized mesoporous magnetite nanoparticles having environmental applications. Chem Solid Mater 2:11–19
31. Seyed Danesh SM, Faghihian H, Shariati S (2018) Sulfonic acid functionalized magnetite nanoporous-KIT-6 for removal of methyl green from aqueous solutions. J Nano Res 52:54–70
32. Rotte NK, Yerramala S, Boniface J, Srikanth VVSS (2014) Equilibrium and kinetics of Safranin O dye adsorption on MgO decked multi- layered graphene. Chem Eng J 258:412–419
33. Zazouli MA, Balarak D, Mahdavi Y (2013) Application of Azolla Filiculoides biomass for 2-Chlorophenol and 4-Chrorophenol removal from aqueous solutions. Iran J Health Sci 1:43–55
34. Ozcan A, Safa Ozcan A (2005) Adsorption of acid Red 57 from aqueous solutions onto surfactant-modified sepiolite. J Hazard Mater B 125:252–259
35. Mohamed F, Abukhadra MR, Shaban M (2018) Removal of safranin dye from water using polypyrrole nanofiber/Zn-Fe layered double hydroxide nanocomposite (Ppy NF/Zn-Fe LDH) of enhanced adsorption and photocatalytic properties. Sci Total Environ 640–641:352–363